ELSEVIER

Inorganica Chimica Acta 229 (1995) 135–142

Inorganica Chimica Acta

Characterization of the isocyanurate complexes [M(cyan-*N*)-$(H_2O)_5$](cyan-*N*)·$2H_2O$ (M = Ni, Co, Mn) compounds that form molecular ribbons in the solid state ☆

Larry R. Falvello *, Isabel Pascual, Milagros Tomás

Department of Inorganic Chemistry and Aragon Materials Science Institute, University of Zaragoza – C.S.I.C., Plaza San Francisco s/n, E-50009 Zaragoza, Spain

Received 24 May 1994; revised 18 August 1994

Abstract

The three isocyanurate complexes [M(cyan-*N*)$(H_2O)_5$](cyan-*N*)·$2H_2O$ (M = Mn (**1**), Co (**2**), Ni (**3**); cyan-*N* = isocyanurate, $C_3H_2N_3O_3^-$, keto isomer) have been prepared and characterized. The complexes are prepared by reaction of $LiC_3H_2N_3O_3$ and $MCl_2·6H_2O$ in water. In the solid state, the compounds exist as the pentaaquamonoisocyanurato transition metal complexes, with a free isocyanurate ion and two free molecules of water per complex. The three compounds are isotypic in the crystalline state, crystallizing in monoclinic space group $P2_1/n$ with $Z = 4$. For compound **1**, $a = 14.038(3)$, $b = 6.693(2)$, $c = 17.813(6)$ Å, $\beta = 97.43(3)°$ and $V = 1659.6(8)$ Å^3. For **2**, $a = 14.017(3)$, $b = 6.612(1)$, $c = 17.067(3)$ Å, $\beta = 97.84(3)°$ and $V = 1567.0(5)$ Å^3. For **3**, $a = 13.965(6)$, $b = 6.623(3)$, $c = 16.997(8)$ Å, $\beta = 98.06(4)°$ and $V = 1557(1)$ Å^3. The bond lengths to the transition metal centers show the expected monotonic decrease on going from manganese to cobalt to nickel. The complexes in the solid state form an extended aggregate of cross-linked molecular ribbons, which are stacked perpendicular to the crystallographic direction [010]. The crystals grow preferentially in the direction of propagation of the molecular ribbons and the direction of stacking. The formation of the supramolecular structure is implicated as a cause of the composition of the transition-metal complexes.

Keywords: Crystal structures; Supramolecular aggregation; Transition metal complexes; Polyfunctional ligand complexes

1. Introduction

The cyanurate and isocyanurate anions, $C_3H_2N_3O_3^-$, possess six functional groups and are thus capable of simultaneously playing two roles in molecular solid-state chemistry. One of these moieties can serve as a ligand in transition-metal complexes while at the same time taking part in stabilizing interactions, such as hydrogen bonds, with a crystalline environment. Crystals of molecular complexes with cyanurate or isocyanurate ligands can thus serve as probes of the balance between the intermolecular forces in a crystal and the intramolecular forces that establish the details of the shape of a molecule, whenever these sets of forces are similar enough that their balance can affect both. Under favorable experimental conditions, such systems can expose the behaviour of a transition-metal complex locked into an extended polymolecular aggregate, since these ligands are able to interact with their surroundings in such a way as to permit the formation of ordered supramolecular aggregates. As part of an ongoing research effort into these effects, we are evaluating candidate systems for molecular solid solution formation. We report here the preparations and structures of three such candidate systems involving the isocyanurate ligand, and the extended solid-state aggregates that they form.

The ligand chemistry of cyanurate and isocyanurate goes back at least as far as the middle of the nineteenth century, when cyanurates of copper were reported [1,2]. Later in that century, elemental stoichiometries were given for a series of cyanurates of magnesium, manganese, cobalt, nickel and zinc [3]. These were prepared from aqueous solutions of metal salts with sodium cyanurate or with cyanuric acid in ammoniacal solution. (At the time of these first studies, the cyclic structures of cyanurate and isocyanurate were of course not known.) In 1972, Taylor [4] reported the preparation of many of the same compounds by reaction of metal

☆ Dedicated to Professor F. Albert Cotton on the occasion of his 65th birthday.

* Corresponding author.

SSDI 0020-1693(94)04238-Q

salts with molten urea. These last two studies established that a wide variety of compounds were to be found in the inorganic chemistry of the cyanurates. The crystal structure of one compound, *trans*-$Cu(NH_3)_2$(cyan-*N*)$_2$, was reported in 1973 [5] (cyan-*N* = isocyanurate, which is the keto tautomer of $C_3H_2N_3O_3^-$, bound through a deprotonated nitrogen atom).

Since that time, preparations and non-crystallographic characterization have been reported for cyanurates of silver [6], lead [7], scandium [8], iron, iridium and bismuth [9], aluminum [10] and zirconium [11]. In addition, the preparations of several of the century-old transition-metal cyanurate compounds have been repeated, including the bis-isocyanurato heptahydrates of cobalt, manganese and nickel [12]. These were characterized by powder diffraction, IR spectroscopy, thermogravimetric analysis and magnetic susceptibility. A crystal structure of the cobalt complex was also reported [13].

We report here a facile preparative route to the complexes [M(cyan-*N*)$(H_2O)_5$](cyan-*N*)$\cdot 2H_2O$, M = Mn (**1**), Co (**2**), Ni (**3**). We have determined, for the first time, the crystal structures of **1** and **3** and have repeated the structure determination of **2** in order to have an accurate basis for comparison. The structures indicate that extended polymolecular aggregation in the solid state is the driving force behind the unusual geometrical arrangement of the metal complex and free isocyanurate anion.

2. Experimental

All reactions were carried out in air. IR spectra were recorded from Nujol mulls between polyethylene film, on a Perkin-Elmer 1730 Fourier-transform spectrophotometer. Elemental analyses were carried out on a Perkin-Elmer 240-B microanalyzer.

Li($C_3H_2N_3O_3$) was prepared by stirring LiOH and $C_3H_3N_3O_3$, in a 1:1 mole ratio, in ethanol for 6 h at room temperature. The colorless solution was partially evaporated, and acetone was added to precipitate the product, which was then filtered and dried with diethyl ether.

All other reagents were used as received.

2.1. Preparation of [M(cyan-N)$(H_2O)_5$](cyan-N)$\cdot 2H_2O$ (M = Mn, (1), Co (2), Ni (3)

Method A. To 20 ml of distilled water were added 0.1 g (0.4 mmol) of $MCl_2\cdot 6H_2O$ and 0.11 g (0.82 mmol) of Li($C_3H_2N_3O_3$) (mole ratio 1:2). The mixture was stirred for 30 min, yielding a powdered solid that was filtered and washed with several aliquots of distilled water, and then allowed to dry in the air.

[Mn(cyan-*N*)$(H_2O)_5$](cyan-*N*)$\cdot 2H_2O$ (**1**). The product was a white powder. Yield 0.158 g (86.2%). *Anal.* Calc for $MnC_6H_{18}N_6O_{13}$: C, 16.48; H, 4.15; N, 19.22. Found: C, 16.76; H, 2.60; N, 19.43%. IR (cm^{-1}): 3600–3000 (vb, s); 1700–1560 (vb, s); 1480–1380 (vb, s); 1095 (m); 555 (s); 415 (s). The sample undergoes a phase change in the solid state at 300 °C, accompanied by changes in the IR spectrum. The IR spectrum, however, does indicate the continued presence of both cyanurate and water. The apparent hydrogen deficiency in the sample analyzed may be a result of partial dehydration.

[Co(cyan-*N*)$(H_2O)_5$](cyan-*N*)$\cdot 2H_2O$ (**2**). The product was a pink powder. Yield 0.158 g (85.3%). *Anal.* Calc. for $CoC_6H_{18}N_6O_{13}$: C, 16.34; H, 4.11; N, 19.05. Found: C, 16.15; H, 3.36; N, 18.93%. IR (cm^{-1}): 3600–3000 (vb, s); 1700–1560 (vb, s); 1480–1380 (vb, s); 1081 (m); 555 (s); 435 (s). On heating in the solid state, the compound changes from pink to mauve at 160 °C, to violet at 170 °C, and to purple at 180 °C, without melting. The IR spectrum of the purple product indicates the presence of both water and cyanurate. The phase change is reversible; the pink complex **2** is restored upon addition of water.

[Ni(cyan-*N*)$(H_2O)_5$](cyan-*N*)$\cdot 2H_2O$ (**3**). Yield of yellowish green powder, 0.156 g (84.3%). *Anal.* Calc. for $NiC_6H_{18}N_6O_{13}$: C, 16.34; H, 4.11; N, 19.06. Found: C, 15.99; H, 4.05; N, 18.96%. IR (cm^{-1}): 3600–3000 (vb, s); 1700–1560 (vb, s); 1480–1380 (vb, s); 1080 (m); 555 (s); 430 (s). On heating in the solid, compound **3** changes from light green to salmon-colored at 240 °C. The IR spectrum of the salmon product indicates that cyanurate and water are still present.

For any of the products prepared by method A, if the powder obtained is washed successively with methanol, ethanol, isopropanol and ether, the water molecules bound to the metal can be replaced by MeOH and EtOH. This process can be monitored though the IR spectra and by the observation of the formation of more deeply colored products. Compounds **1**, **2** and **3** are soluble only in very polar solvents such as DMSO and concentrated NH_3, which are capable of destroying the network of hydrogen bonds in the solid (vide infra), and which substitute the coordinated water.

The crystals that were used in the X-ray diffraction analyses were obtained by partial evaporation and subsequent cooling of the mother liquids from the preparations by method A.

Method B. A crop of crystalline plates of any of these products can be obtained by slow diffusion of a solution of Li($C_3H_2N_3O_3$) in EtOH/H_2O (50:50) into a saturated solution of $MCl_2\cdot 6H_2O$ in i-PrOH. This procedure yields the solid product within 5 days at room temperature.

2.2. Crystal structure determinations

2.2.1. General procedure

All of the crystals used for X-ray diffraction analysis were thin plates. Crystals of the manganese complex, **1**, are colorless, those of the cobalt complex, **2**, are pink, and the crystals of the nickel compound, **3**, are light green. Each of the crystals used was affixed to the end of a glass fiber with epoxy. All data were taken at room temperature. Routine procedures were used for cell and orientation matrix determination, and in all cases the lattice parameters were verified by normal-beam oscillation photography. During intensity data collection for each sample, three monitor reflections were measured after every two hours to check for instrument and/or crystal instability. No observable changes occurred in the intensities of these reflections. Data reduction and structure solution were carried out on a Local Area VAX cluster (VMS V5.5) by the program REDU4 Rev. 7.03 (Stöe) using the commercial package SHELXTL-PLUS [14], and the least-squares refinements were done by the program Shelxl-93 [15]. For all of the structures, all data with positive measured intensities were used in the final refinements. In each case, the data used in the refinement were F_o^2. Crystal data and other parameters relevant to data collection and structure refinement are given in Table 1.

2.2.2. Crystal structure of $[Mn(cyan\text{-}N)(H_2O)_5](cyan\text{-}N)\cdot 2H_2O$ (1)

Intensities were measured for a quarter-sphere of reflections. Azimuthal scans (ψ-scans) of six scattering vectors with Eulerian angle χ near 90° were used as the basis of an absorption correction. The structure was solved by direct methods and refined by full-matrix least-squares. All non-hydrogen atoms were refined anisotropically. Hydrogen atoms were located in difference Fourier maps and refined freely, each with its own isotropic displacement parameter. In the final least-squares cycle, 307 parameters were fitted to 2512 unique reflection data, for a data-to-parameter ratio of 8.2. The refinement converged with the residuals given in Table 1. Atomic positional and equivalent isotropic displacement parameters are given in Table 2, and selected bond distances and angles are given in Table 3.

2.2.3. Crystal structure of $[Co(cyan\text{-}N)(H_2O)_5](cyan\text{-}N)\cdot 2H_2O$ (2)

Intensities were measured for a quadrant of reflections which, after averaging of equivalent data, yielded 2125 positive values of F_o^2 for use in the structure refinement. Starting coordinates for non-hydrogen atoms were taken from the structure of complex **1**. Hydrogen atoms were located in a difference Fourier map, and were refined freely. The data-to-parameter ratio in the final least-squares cycle was 6.9. The refinement converged with the residuals given in Table 1. Atomic parameters for **2** are given in Table 4, and selected bond distances and angles are given in Table 5.

2.2.4. Crystal structure of $[Ni(cyan\text{-}N)(H_2O)_5](cyan\text{-}N)\cdot 2H_2O$ (3)

Crystals of the nickel complex were thin pinacoids, and all of the samples examined were found to comprise more than one crystal. In the end, we took data from a very thin crystal (smallest dimension 0.023 mm) to which was attached one or more minor satellites. The satellites were visible only in axial photography, and not by visible-light microscopy. Some adverse effects evidently caused by the satellite(s) were seen in the refinement of the hydrogen atoms (see below), but otherwise the structure determination did not present any special problems. A diffractometer failure that caused a delay during the course of data collection apparently left no adverse effects either, as there was no crystal decay.

The initial structural model consisted of coordinates taken from the structure of compound **1**. All non-hydrogen atoms were refined anisotropically. Hydrogen atoms were visible in a difference map, but the positions of only some of them were considered acceptable for inclusion in the structural model. The remainder were included at idealized positions. Four of the hydrogen atoms were well enough behaved under refinement to be refined completely freely, with independent isotropic displacement parameters. A common isotropic displacement parameter was refined for the other 14 hydrogen atoms of the asymmetric unit. Loose observational restraints were applied to six O–H and N–H distances, and in addition, observational restraints were used to keep the hydrogen atoms of the free cyanurate in the plane of the group. In all, 294 variable parameters were refined to 2715 reflection data and 8 observational restraints, for an observation-to-parameter ratio of 9.3. The refinement converged with the residuals given in Table 1. Atomic coordinates for complex **3** are given in Table 6, and selected distances and angles are listed in Table 7.

3. Results and discussion

3.1. Molecular shapes

The three structures are essentially isotypic and can serve as a basis for comparison of the geometries about the Mn, Co and Ni centers. In these pentaaqua isocyanurate complexes we observe the expected monotonic decrease in bond lengths, bond for bond, on going from manganese to cobalt to nickel (see Tables 3, 5 and 7). The trend in bond lengths for the entire first transition

Table 1
Crystal data for $[M(cyan\text{-}N)(H_2O)_5](cyan\text{-}N)\cdot 2H_2O$, M = Mn (**1**), Co (**2**), Ni (**3**)

	1	**2**	**3**
Formula	$MnC_6H_{18}N_6O_{13}$	$CoC_6H_{18}N_6O_{13}$	$NiC_6H_{18}N_6O_{13}$
Formula weight	437.20	441.19	440.97
Space group	$P2_1/n$	$P2_1/n$	$P2_1/n$
Systematic absences	$(0k0)$: $k\neq 2n$	$(0k0)$: $k\neq 2n$	$(0k0)$: $k\neq 2n$
	$(h0l)$: $h+l\neq 2n$	$(h0l)$: $h+l\neq 2n$	$(h0l)$: $h+l\neq 2n$
a (Å)	14.038(3)	14.017(3)	13.965(6)
b (Å)	6.693(2)	6.612(1)	6.623(3)
c (Å)	17.813(6)	17.067(3)	16.997(8)
β (°)	97.43(3)	97.84(3)	98.06(4)
V (Å^3)	1659.6(8)	1567.0(5)	1557(1)
Z	4	4	4
D_{calc} (g cm^{-3})	1.750	1.870	1.882
Crystal size (mm)	0.67×0.40×0.02	0.28×0.26×0.02	0.60×0.34×0.02
μ (Mo Kα) (cm^{-1})	8.77	11.82	13.34
Transmission factors: max., min.	0.88, 0.66	0.98, 0.78	1.00, 0.78
Data collection instrument	Stoe AED-2	Stoe AED-2	Stoe AED-2
Radiation (graphite monochromated), λ (Å)	Mo Kα, 0.71073	Mo Kα, 0.71073	Mo Kα, 0.71073
Orientation reflections: no., range, 2θ (°)	24, 26–30	24, 26–30	19, 26–30
Temperature (K)	293±2	298±2	293±2
Scan method	ω–θ	ω–θ	ω–θ
Data collection range, 2θ (°)	4–50	4–48	4–50
Index ranges	$+h,+k,\pm l$	$+h,+k,\pm l$	$+h,+k,\pm l$
No. data: total, unique	2898, 2644	2461, 2357	2715, 2500
No. data with $F_o^2 \geq 2\sigma(F_o^2)$	2225	1678	1703
No. and type of data used in refinement	$2512F^2 \geq 0$	$2125F^2 \geq 0$	$2235F^2 \geq 0$
No. restraints	0	0	8
No. parameters refined	307	307	294
$wR2$ [a]	0.0846	0.1070	0.1572
$R1$ [b] (for $F_o^2 \geq \sigma(F_o^2)$)	0.0333	0.0426	0.0561
Weighting parameters: g_1, g_2 [c]	0.0516, 0.28	0.0542, 0.34	0.0828, 0.00
Quality of fit: unrestrained [d], restrained [e]	1.070	1.077	1.182, 1.181
$wR(F)$ (for $F_o \geq 4\sigma(F_o)$) [f,g]	0.0431	0.0526	0.0716
Mean, max. |shift/e.s.d.|, final cycle	0.001, 0.005	0.002, 0.020	0.009, 0.169
Largest difference peak and trough (e Å^{-3})	0.41, −0.52	0.31, −0.42	0.55, −0.60

[a] $wR2 = [\Sigma w(F_o^2 - F_c^2)^2 / \Sigma w(F_o^2)^2]^{1/2}$.
[b] $R1 = \Sigma \| F_o | - | F_c \| / \Sigma | F_o |$.
[c] $w = [\sigma^2(F_o^2) + (g_1 P)^2 + g_2 P]^{-1}$; $P = [\max(F_o^2; 0) + 2F_c^2]/3$.
[d] Quality of fit $= [\Sigma w(F_o^2 - F_c^2)^2 / (N_{obs} - N_{param})]^{1/2}$.
[e] Restrained $QOF = \left[\frac{\Sigma w(F_o^2 - F_c^2)^2 + \Sigma w(Y_{target} - Y_{calc})^2}{(N_{reflec} + N_{restraints} - N_{param})} \right]^{1/2}$
[f] $wR(F) = [\Sigma w(F_o - F_c)^2 / \Sigma w(F_o)^2]^{1/2}$; $w^{-1} = [\sigma^2(F_o) + 0.001F_o^2]$.
[g] The values of $wR(F)$ were calculated from the observed structure factors and the final structural parameters. They are given here only for the purpose of comparison. The statistically valid residuals from these refinements are $wR2$ and quality of fit.

series has recently been explored experimentally in two series of hexaaqua complexes [16]; the experimental results in that case, as in the present, agree well with the predictions of theory, that there should be maxima in the distances to manganese and zinc, and a minimum at nickel.

3.2. Hydrogen bonding and molecular aggregation

The crystallographic asymmetric unit in each of the present structures consists of one unit of the cationic complex $[M(cyan\text{-}N)(H_2O)_5]^+$, one free isocyanurate ion and two molecules of water. The atom naming scheme is shown in Fig. 1. The structures display two striking features – the presence of extensive hydrogen bonding and the fact that only one of the two isocyanurate entities is bound to the central metal atom. As we shall describe presently, these two features are related.

The hydrogen-bonding pattern in these structures is essentially complete. That is to say, all eighteen unique hydrogen atoms participate in hydrogen bonds, and the pattern of interactions extends in all three dimensions. Of the fourteen potential hydrogen-bond acceptors in the asymmetric unit, comprising the deprotonated nitrogen atom N(21) of the uncoordinated isocyanurate

Table 2
Atomic coordinates ($\times 10^4$) and equivalent isotropic displacement parameters ($Å^2 \times 10^3$) and their e.s.d.s for [Mn(cyan-*N*)$(H_2O)_5$](cyan-*N*)·$2H_2O$ (**1**) [a]

	x	*y*	*z*	U_{eq}
Mn(1)	4418(1)	1797(1)	6785(1)	21(1)
O(1)	3640(1)	3991(3)	7413(1)	27(1)
O(2)	4979(1)	4451(3)	6206(1)	28(1)
O(3)	3693(1)	−601(3)	7293(1)	32(1)
O(4)	5027(2)	−128(3)	5965(1)	36(1)
O(5)	3124(1)	1872(3)	5911(1)	39(1)
N(11)	5686(1)	1823(3)	7728(1)	19(1)
C(12)	6572(2)	1928(3)	7499(1)	21(1)
O(12)	6709(1)	1783(3)	6808(1)	31(1)
N(13)	7364(2)	2193(3)	8059(1)	26(1)
C(14)	7315(2)	2477(4)	8833(1)	25(1)
O(14)	8029(1)	2817(3)	9302(1)	40(1)
N(15)	6408(1)	2370(3)	9032(1)	23(1)
C(16)	5594(2)	2003(3)	8500(1)	19(1)
O(16)	4812(1)	1851(3)	8754(1)	28(1)
N(21)	187(1)	1835(3)	6624(1)	21(1)
C(22)	300(2)	2137(4)	5866(1)	22(1)
O(22)	1098(1)	2089(3)	5629(1)	36(1)
N(23)	−497(1)	2501(3)	5325(1)	25(1)
C(24)	−1408(2)	2598(4)	5511(1)	23(1)
O(24)	−2102(1)	2946(3)	5028(1)	41(1)
N(25)	−1485(1)	2299(3)	6281(1)	23(1)
C(26)	−702(2)	1911(3)	6840(1)	19(1)
O(26)	−864(1)	1658(3)	7521(1)	26(1)
O(31)	4057(1)	6862(3)	5069(1)	33(1)
O(41)	2563(1)	1641(3)	8435(1)	32(1)

[a] The equivalent isotropic displacement parameter, U_{eq}, is calculated as: $U_{eq} = \frac{1}{3}\Sigma_{ij} U_{ij} \boldsymbol{a}_i \cdot \boldsymbol{a}_j \boldsymbol{a}_i^* \boldsymbol{a}_j^*$.

Table 3
Selected bond distances (Å) and angles (°) and their e.s.d.s for [Mn(cyan-*N*)$(H_2O)_5$](cyan-*N*)·$2H_2O$ (**1**)

Mn(1)–O(3)	2.161(2)	Mn(1)–O(5)	2.235(2)
Mn(1)–O(4)	2.201(2)	Mn(1)–O(2)	2.247(2)
Mn(1)–O(1)	2.218(2)	Mn(1)–N(11)	2.284(2)
O(3)–Mn(1)–O(4)	95.04(8)	O(1)–Mn(1)–O(2)	86.15(7)
O(3)–Mn(1)–O(1)	89.47(8)	O(5)–Mn(1)–O(2)	87.95(8)
O(4)–Mn(1)–O(1)	168.87(7)	O(3)–Mn(1)–N(11)	93.55(8)
O(3)–Mn(1)–O(5)	85.64(8)	O(4)–Mn(1)–N(11)	99.21(7)
O(4)–Mn(1)–O(5)	84.37(8)	O(1)–Mn(1)–N(11)	90.64(7)
O(1)–Mn(1)–O(5)	85.84(8)	O(5)–Mn(1)–N(11)	176.39(7)
O(3)–Mn(1)–O(2)	172.48(7)	O(2)–Mn(1)–N(11)	92.61(7)
O(4)–Mn(1)–O(2)	88.23(8)		

Table 4
Atomic coordinates ($\times 10^4$) and equivalent isotropic displacement parameters ($Å^2 \times 10^3$) and their e.s.d.s for [Co(cyan-*N*)$(H_2O)_5$](cyan-*N*)·$2H_2O$ (**2**) [a]

	x	*y*	*z*	U_{eq}
Co(1)	4380(1)	1874(1)	6789(1)	21(1)
O(1)	3660(3)	3970(6)	7404(3)	27(1)
O(2)	4958(3)	4366(6)	6226(2)	28(1)
O(3)	3709(3)	−444(6)	7292(3)	29(1)
O(4)	4980(3)	−3(8)	6018(3)	38(1)
O(5)	3130(3)	1917(8)	5921(2)	40(1)
N(11)	5639(3)	1839(6)	7696(2)	19(1)
C(12)	6533(3)	1905(8)	7474(3)	22(1)
O(12)	6677(2)	1732(6)	6777(2)	31(1)
N(13)	7323(3)	2137(7)	8047(2)	27(1)
C(14)	7282(4)	2428(8)	8828(3)	29(1)
O(14)	7998(3)	2732(7)	9299(2)	42(1)
N(15)	6368(3)	2348(6)	9017(2)	25(1)
O(16)	4770(2)	1892(6)	8733(2)	28(1)
C(16)	5543(3)	2006(7)	8475(3)	19(1)
N(21)	164(3)	1869(6)	6638(2)	21(1)
C(22)	285(3)	2158(8)	5876(3)	23(1)
O(22)	1081(2)	2115(7)	5640(2)	37(1)
N(23)	−520(3)	2523(6)	5322(3)	26(1)
C(24)	−1431(4)	2588(7)	5509(3)	22(1)
O(24)	−2127(2)	2921(7)	5014(2)	41(1)
N(25)	−1499(3)	2294(6)	6281(2)	24(1)
C(26)	−725(3)	1925(7)	6848(3)	21(1)
O(26)	−890(2)	1664(6)	7536(2)	28(1)
O(31)	4092(3)	6925(7)	5090(2)	34(1)
O(41)	2534(2)	1717(6)	8412(2)	30(1)

[a] The equivalent isotropic displacement parameter, U_{eq}, is calculated as: $U_{eq} = \frac{1}{3}\Sigma_{ij} U_{ij} \boldsymbol{a}_i \cdot \boldsymbol{a}_j \boldsymbol{a}_i^* \boldsymbol{a}_j^*$.

Table 5
Selected bond distances (Å) and angles (°) and their e.s.d.s for [Co(cyan-*N*)$(H_2O)_5$](cyan-*N*)·$2H_2O$ (**2**)

Co(1)–O(3)	2.048(4)	Co(1)–O(2)	2.123(4)
Co(1)–O(4)	2.068(4)	Co(1)–O(5)	2.135(4)
Co(1)–O(1)	2.081(4)	Co(1)–N(11)	2.183(4)
O(3)–Co(1)–O(4)	93.8(2)	O(1)–Co(1)–O(5)	86.1(2)
O(3)–Co(1)–O(1)	90.3(2)	O(2)–Co(1)–O(5)	90.2(2)
O(4)–Co(1)–O(1)	171.0(2)	O(3)–Co(1)–N(11)	93.9(2)
O(3)–Co(1)–O(2)	175.1(2)	O(4)–Co(1)–N(11)	94.9(2)
O(4)–Co(1)–O(2)	88.0(2)	O(1)–Co(1)–N(11)	92.8(2)
O(1)–Co(1)–O(2)	87.3(2)	O(2)–Co(1)–N(11)	90.5(2)
O(3)–Co(1)–O(5)	85.4(2)	O(5)–Co(1)–N(11)	178.7(2)
O(4)–Co(1)–O(5)	86.2(2)		

and the thirteen unique oxygen atoms, twelve serve as acceptors in hydrogen bonds. We do note that the hydrogen bonds observed here are generally longer and less linear than those found in organic molecular structures; this may reflect a compromise in the present structures among all of the factors affecting packing. There is one bifurcated hydrogen bond, in which one of the hydrogen atoms (H(41) in our naming scheme) of the aquo ligand at O(4) is the donor. This interaction gives rise to a minor difference among the three structures. In the structure of the manganese compound, **1**, the bifurcated hydrogen bond has the characteristic geometry of such an entity – slightly longer distances (2.922(3) and 3.146(3) Å) and bent angles of 124(3) and 146(3)° for the two simultaneous donor···acceptor interactions. In the cobalt and nickel complexes, there is a foreshortening of one of the distances and an elongation of the other; but the angular relationships retain the characteristics of the bifurcated hydrogen bond. So, for example, in the structure of the cobalt

Table 6
Atomic coordinates ($\times 10^4$) and equivalent isotropic displacement parameters ($Å^2 \times 10^3$) and their e.s.d.s for [Ni(cyan-*N*)$(H_2O)_5$](cyan-*N*)·$2H_2O$ (**3**) [a]

	x	*y*	*z*	U_{eq}
Ni(1)	4377(1)	1902(1)	6792(1)	19(1)
O(1)	3663(4)	3969(7)	7400(3)	25(1)
O(2)	4953(4)	4314(8)	6231(3)	27(1)
O(3)	3704(4)	−387(8)	7303(3)	29(1)
O(4)	4973(4)	−2(9)	6040(4)	39(2)
O(5)	3145(4)	1963(10)	5942(3)	38(1)
N(11)	5616(4)	1843(9)	7692(3)	18(1)
C(12)	6507(4)	1880(10)	7470(4)	20(1)
O(12)	6662(3)	1713(8)	6774(3)	29(1)
N(13)	7303(4)	2118(10)	8043(3)	26(1)
C(14)	7277(5)	2410(11)	8834(4)	27(2)
O(14)	7991(4)	2701(9)	9307(3)	41(2)
N(15)	6359(4)	2336(8)	9013(3)	24(1)
O(16)	4747(3)	1879(8)	8728(3)	28(1)
C(16)	5523(5)	1986(10)	8467(4)	22(1)
N(21)	168(4)	1854(9)	6644(3)	21(1)
C(22)	284(5)	2154(10)	5871(4)	22(2)
O(22)	1089(3)	2130(9)	5637(3)	33(1)
N(23)	−508(4)	2532(9)	5326(3)	27(1)
C(24)	−1436(5)	2592(10)	5496(4)	21(2)
O(24)	−2135(3)	2933(10)	5010(3)	41(1)
N(25)	−1504(4)	2290(9)	6282(3)	23(1)
C(26)	−721(5)	1900(9)	6854(4)	19(1)
O(26)	−892(3)	1618(8)	7543(2)	27(1)
O(31)	4093(4)	6922(10)	5099(3)	32(1)
O(41)	2515(4)	1744(9)	8404(3)	32(1)

[a] The equivalent isotropic displacement parameters, U_{eq}, is calculated as: $U_{eq} = \frac{1}{3}\Sigma_{ij} U_{ij} \boldsymbol{a}_i \cdot \boldsymbol{a}_j a_i^* a_j^*$.

Table 7
Selected bond distances (Å) and angles (°) and their e.s.d.s for [Ni(cyan-*N*)$(H_2O)_5$](cyan-*N*)·$2H_2O$ (**3**)

Ni(1)–O(3)	2.041(5)	Ni(1)–O(2)	2.079(5)
Ni(1)–O(4)	2.053(6)	Ni(1)–O(5)	2.086(5)
Ni(1)–O(1)	2.056(5)	Ni(1)–N(11)	2.143(5)
O(3)–Ni(1)–O(4)	93.4(2)	O(1)–Ni(1)–O(5)	85.7(2)
O(3)–Ni(1)–O(1)	89.7(2)	O(2)–Ni(1)–O(5)	90.1(2)
O(4)–Ni(1)–O(1)	171.8(2)	O(3)–Ni(1)–N(11)	93.2(2)
O(3)–Ni(1)–O(2)	175.4(2)	O(4)–Ni(1)–N(11)	94.4(2)
O(4)–Ni(1)–O(2)	88.3(2)	O(1)–Ni(1)–N(11)	93.0(2)
O(1)–Ni(1)–O(2)	88.0(2)	O(2)–Ni(1)–N(11)	90.9(2)
O(3)–Ni(1)–O(5)	85.7(2)	O(5)–Ni(1)–N(11)	178.3(2)
O(4)–Ni(1)–O(5)	87.0(2)		

compound, **2**, the distances are 2.795(6) and 3.316(6) Å, and the angles at hydrogen are 138(5) and 136(5)°. In the nickel compound, **3**, the donor···acceptor distances for this interaction are 2.754(7) and 3.349(8) Å. (In the case of the nickel compound, the hydrogen atom positions were subject to restraints in the refinement and thus cannot be used for detailed comparisons of the H-bond angles.) The extent to which the minor component of the bifurcated interaction contributes to the stability of the crystals of compounds

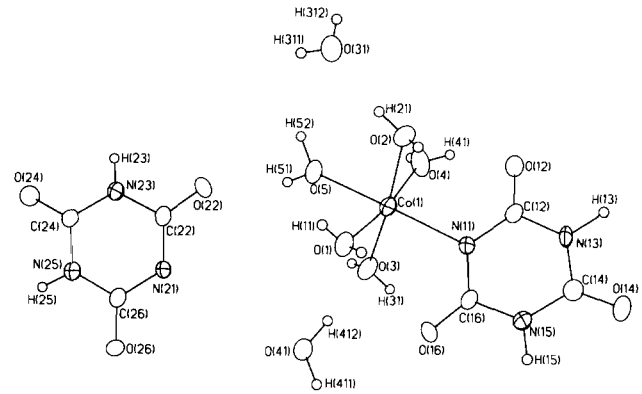

Fig. 1. Displacement ellipsoid plot of one asymmetric unit of [Co(cyan-*N*)$(H_2O)_5$](cyan-*N*)·$2H_2O$ (**2**) showing the atom naming scheme. Non-hydrogen atoms are represented by their 50% probability ellipsoids.

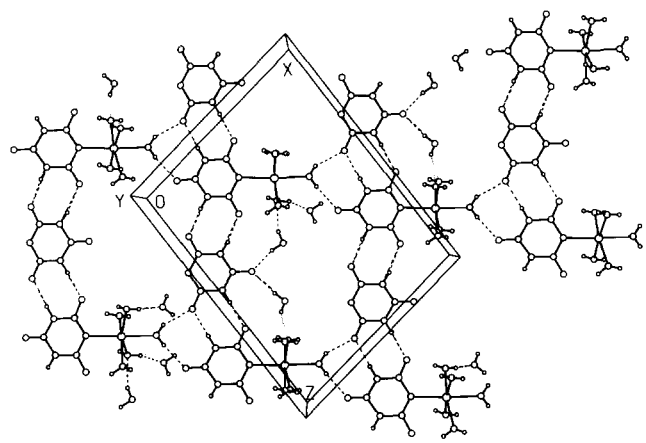

Fig. 2. Drawing of the extended crystal structure of [Mn(cyan-*N*)$(H_2O)_5$](cyan-*N*)·$2H_2O$ (**1**) viewed along the crystallographic *b*-axis.

2 and **3** is open to question. It seems unlikely that the longer contacts in these two cases could provide much stability to the structure. We prefer not to deem them hydrogen bonds. The difference between the structure of **1**, on the one hand, and **2** and **3**, on the other, appears to be caused by packing strain and is not the result of any fundamental structural difference. There is also a trifurcated hydrogen bond, in which the free water molecule O(41) is the donor. The three acceptor atoms are the ligated aquo oxygen atoms O(1) and O(3) and the proximal *ortho*-carbonyl oxygen atom of the ligated isocyanurate moiety.

The hydrogen-bonding pattern mediates an extended system of supramolecular aggregation in the solid state, which can best be described as a cross-linked set of parallel molecular ribbons. Fig. 2 is a drawing of the extended crystal structure, viewed along the *b*-axis. As Fig. 2 shows, the isocyanurate ligand and the free isocyanurate ion take part in base pairing to form a molecular ribbon that extends for the entirety of the crystal, being propagated along the vector [1,0,−1].

These ribbons are cross-linked in the (010) plane, the plane of the picture in Fig. 2, by the rest of the $[(M(cyan\text{-}N)(H_2O)_5]^+$ complex. So the isocyanurate ligand of the complex participates in a ribbon, while the aquo ligand *trans* to it at O(5) makes hydrogen bonds to both a bound and a free isocyanurate of the neighboring ribbon. The spacing between ribbons is roughly 10 Å. It varies slightly from structure to structure. Each ribbon has a pseudo-two-fold axis of symmetry lying midway between adjoining isocyanurate groups.

Layers of these molecular ribbons are stacked perpendicular to the crystallographic *y*-axis. Adjoining layers are related by the crystallographic 2_1 screw axis, and are stacked in such a way that the layers are nearly eclipsed. The stacking interval in one-half of the b lattice repeat, or approximately 3.3 Å in each case. The precise lattice parameters are given for each of the three complexes in Table 1. The stacking separation is similar to that in graphite (3.4 Å), and indicates a stabilizing van der Waals' interaction between successive layers. Fig. 3 is a drawing of the extended structure viewed perpendicular to the *y*-axis. It gives a side-one view of the layering of the polymolecular ribbons. As can be appreciated in the Figure, there is cross-linking between layers as well. This is mediated by hydrogen bonding in which the aquo ligands of the equatorial plane of the complex – that is, O(1), O(2), O(3) and O(4) – serve as donors. A third view of the extended structure – on the plane (−1,0,1) – is shown in Fig. 4. The molecular ribbons are seen end-on, and the cross-linking between layers is clearly visible.

Some recent reports in the literature have indicated the importance of hydrogen bonding in mediating molecular aggregation with important consequences in organic synthesis [17] and with potential import in crystal engineering [18,19]. It appears that in the present isocyanurate complexes the hydrogen bonding is the motive force behind even the nature of the transition-metal complex that crystallizes. A simple synthetic procedure such as the one used to produce these compounds might be expected to yield complexes with

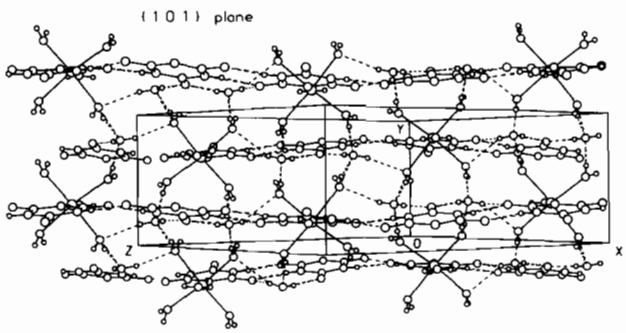

Fig. 3. Drawing of the extended crystal structure of $[Mn(cyan\text{-}N)(H_2O)_5](cyan\text{-}N)\cdot 2H_2O$ (**1**) viewed in the plane (101), showing the stacking of molecular ribbons.

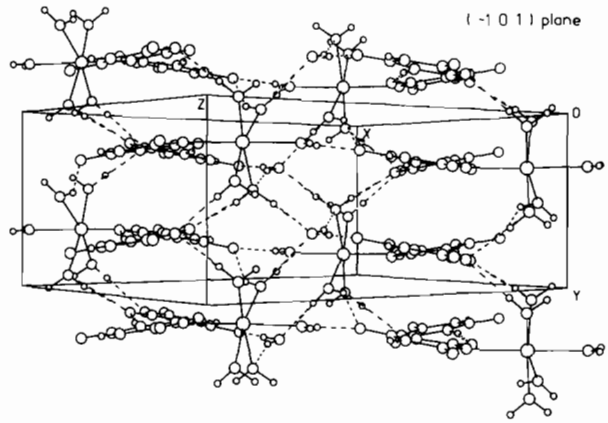

Fig. 4. A third view of the packing in the structure of $[Mn(cyan\text{-}N)(H_2O)_5](cyan\text{-}N)\cdot 2H_2O$ (**1**) drawn on the plane (−1,0,1). The molecular ribbons are seen end-on.

a pair of isocyanurate ligands *trans* to each other, as is seen with other aqua complexes containing polyfunctional ligands such as saccharinate [20] and nicotinate [21]. Instead, we obtain in the crystalline state and in good yield, complexes of the type $[M(cyan\text{-}N)(H_2O)_5]^+$.

In searching for possible explanations for the stoichiometry that emerges in the solid state for the present compounds, we note (Fig. 2) that both the axial aqua ligand and the 'free' cyanurate moiety are key elements in the aggregate extended structure. The axial water is necessary for the cross-linking of molecular ribbons in the solid; and of course the uncoordinated cyanurate forms part of the ribbon itself. One could envisage other arrangements, based for example upon the molecular entity *trans*-$[M(cyan\text{-}N)_2(H_2O)_4]$, which would be stable. It would be unduly speculative at this point, however, to attempt a detailed comparison of the structure that in fact emerges, with others that might have been expected to emerge. In addition, we do not at present have concrete evidence regarding the structures present in the solution from which the crystals are grown. It would be useful to know whether hydrogen-bonded aggregates such as ribbons are present to any appreciable extent prior to crystallization.

As further evidence that it is the complex network of hydrogen bonding and ring stacking that determines the stoichiometry of the complexes **1**, **2** and **3**, we cite a complex of nickel that we have prepared and structurally characterized, in which the aquo ligands of the present system are replaced by NH_3 [22]. In the crystal structure there is a single hydrogen bond instead of the extended pattern seen in the present compounds; and the nickel complex is that expected on the basis of chemical intuition, namely *trans*-$[Ni(cyan\text{-}N)_2(NH_3)_4]$. Its structure and the manner in which it crystallizes reinforce our conclusion about the present systems.

3.3. Crystal morphology

Crystals of **1**, **2** and **3** were all thin plates, for which the prominent face in all cases was (101). The (101) plane is the plane of the drawing in Fig. 3. It is perpendicular to the plane of Fig. 2, and intersects a vertical line in that Figure. Thus, the crystals grew preferentially in two directions, namely the direction of propagation of the molecular ribbon, and the direction of stacking of the ribbons. The direction of cross-linking in the plane of Fig. 2 did not turn out to be a preferential growth direction. Since the crystals were all quite stable, we assume that the two preferred directions of growth simply grew faster than the third, and not that there was any strain or other impediment to growth in the direction of cross-linking. As the crystals at hand were sufficient for our analyses, we did not attempt to grow larger samples.

4. Conclusions

Cyanuric acid itself has been shown capable of forming intermolecular complexes that give rise to extended aggregation in the solid state [17,23,24], including aggregation based on Watson–Crick base pairing. The steric and electrostatic similarity of isocyanuric acid to the pyrimidine bases confers to it a natural capacity for such interaction. We see in the crystal structures of the compounds $[M(cyan\text{-}N)(H_2O)_5](cyan\text{-}N)\cdot 2H_2O$ reported here, that the propensity for aggregation can even supersede the capacity for this moiety to serve as a ligand to a transition-metal center.

5. Supplementary material

Listings of anisotropic displacement parameters, hydrogen atom coordinates, bond distances, bond angles, hydrogen-bonding interactions, and observed and calculated structure factors for the crystal structures of **1**, **2** and **3**, and displacement ellipsoid drawings of the structures of **1** and **3**, are available from the authors on request.

Acknowledgements

Financial support from the Comisión Interministerial de Ciencia y Tecnología, Spain (Grant number PB92-0360) is gratefully acknowledged. The authors thank Professor Juan Forniés for invaluable logistical support.

References

[1] F. Wöhler, *Justus Liebigs Ann. Chem., 62* (1847) 241.
[2] G. Wiedermann, *Justus Liebigs Ann. Chem., 68* (1848) 324.
[3] A. Claus and P. Putensen, *J. Prakt. Chem., 38* (1888) 208.
[4] R.M. Taylor, *Z. Anorg. Allg. Chem., 390* (1972) 85.
[5] P.G. Slade, M. Raupach and E.W. Radoslovich, *Acta Crystallogr., Sect. B., 29* (1973) 279.
[6] (a) G.B. Seifer, N.A. Chumaevskii, N.A. Minaeva and Z.A. Tarasova, *Zh. Neorg. Khim., 35* (1990) 2527; (b) G.B. Seifer and Z.A. Tarasova, *Zh. Neorg. Khim., 34* (1989) 1840; (c) Citations to these and other papers cited subsequently from *Zh. Neorg. Khim.* and *Koord. Khim.* are taken from *Chemical Abstracts.* The papers were unavailable to us. We give the citations and abstracted information as a service to the reader.
[7] G.B. Seifer and Z.A. Tarasova, *Zh. Neorg. Khim., 36* (1991) 1693.
[8] G.B. Seifer and Z.A. Tarasova, *Zh. Neorg. Khim., 32* (1987) 207.
[9] G.B. Seifer and N.A. Chumaevskii, N.A. Minaeva and Z.A. Tarasova, *Zh. Neorg. Khim., 33* (1988) 2555.
[10] (a) G.B. Seifer, N.A. Minaeva and Z.A. Tarasova, *Zh. Neorg. Khim., 32* (1987) 307; (b) G.B. Seifer and Z.A. Tarasova, *Zh. Neorg. Khim., 31* (1986) 1559.
[11] G.B. Seifer, N.A. Minaeva and Z.A. Tarasova, *Koord. Khim., 17* (1991) 1478.
[12] M.Z. Branzburg, T.F. Sysoeva, N.F. Shugal, N.M. Dyatlova, V.M. Agre and M.Z. Gurevich, *Koord. Khim., 12* (1986) 1658.
[13] V.M. Agre, T.F. Sysoeva, V.K. Trunov, M.Z. Gurevich and M.Z. Branzburg, *Koord. Khim., 12* (1986) 122.
[14] *SHELXTL-PLUS,* Release 4.21/V, Siemens Analytical X-ray Instruments, Inc., Madison, WI, USA, 1990.
[15] (a) G.M. Sheldrick, *Shelxl-93,* FORTRAN-77 program for the refinement of crystal structures from diffraction data, University of Göttingen, Germany, 1993; (b) G.M. Sheldrick, *J. Appl. Crystallogr.,* (1994), in preparation.
[16] F.A. Cotton, L.M. Daniels, C.A. Murillo and J.F. Quesada, *Inorg. Chem., 32* (1993) 4861.
[17] J.P. Mathias, C.T. Seto, E.E. Simanek and G.M. Whitesides, *J. Am. Chem. Soc., 116* (1994) 1725, and refs. therein.
[18] V.A. Russell, M.C. Etter and M.D. Ward, *J. Am. Chem. Soc., 116* (1994) 1941, and refs. therein.
[19] C.B. Aakeröy and K.R. Sneddon, *Chem. Soc. Rev., 22* (1993) 397.
[20] (a) S.Z. Haider, K.M.A. Malik, K.J. Ahmed, H. Hess, H. Riffel and M.B. Hursthouse, *Inorg. Chim. Acta, 72* (1983) 21; (b) F.A. Cotton, G.E. Lewis, C.A. Murillo, W. Schwotzer and G. Valle, *Inorg. Chem., 23* (1984) 4038.
[21] (a) M. Biagini Cingi, P. Domiano, C. Guastini, A. Musatti and M. Nardelli, *Gazz. Chim. Ital., 101* (1971) 455; (b) W.E. Broderick, M.R. Pressprich, U. Geiser, R.D. Willett and J.I. Legg, *Inorg. Chem., 25* (1986) 3372; (c) J.A. Cooper, B.F. Anderson, P.D. Buckler and L.F. Blackwell, *Inorg. Chim. Acta, 91* (1984) 1.
[22] I. Pascual, unpublished results.
[23] H.-S. Shieh and D. Voet, *Acta Crystallogr., Sect. B, 32* (1976) 2354.
[24] A. Kutoglu and E. Hellmer, *Acta Crystallogr., Sect. B, 34* (1978) 1617.